J. Materials, Conc. Struct., Pavements, JSCE, No.634／V-45, 337-348, 1999 November

ANALYSIS OF THE RC COLUMNS UNDER PURE TORSION USING THE MODIFIED LATTICE MODEL IN THREE DIMENTIONS

Fawzy Mohamed EL-BEHAIRY[1], Junichiro NIWA[2] and Tada-aki TANABE[3]

[1]Member of JSCE, Dr. of Eng., Technical Research Institute, Maeda Corporation
(Fujimi 2-10-26, Chiyoda-ku, Tokyo 102-8151, Japan)
[2]Member of JSCE, Dr. of Eng., Professor, Dept. of Civil Eng., Tokyo Institute of Technology
(Ookayama 2-12-1, Meguro-ku, Tokyo 152-8552, Japan)
[3]Fellow of JSCE, Dr. of Eng., Professor, Dept. of Civil Eng., Nagoya University
(Furo-cho, Chikusa-ku, Nagoya 464-01, Japan)

The physical understanding and the numerical simulation of the characteristics of R.C. columns have been the focus of intensive efforts. Structural systems which are subjected to any kind of loads become quite difficult to analyse rigorously in their original physical forms, especially when the degree of freedom becomes so large. So in this work, the Modified Lattice Model, which was previously modified by the authors in two dimensions, is extended to the three dimensions. The reinforced concrete column under pure torsion is chosen as a material subject to check the suggested model in 3-D. The applicability of the suggested model in 3-D is examined successfully in comparison with many existing experimental data.

Key Words: *3-D lattice model, arch element, total potential energy, torsion stress, aspect ratio, softening concrete*

1. INTRODUCTION

To capture the shear resisting mechanism of reinforced concrete columns, such as the initiation of diagonal cracking, yielding of reinforcement and crushing of web concrete, and also to establish a particular torsion-resisting model, the Lattice model in 2-D[6), 9)] has been developed to 3-D domain. The calculation procedures using 3-D Lattice Model are rather simple and worthwhile to be investigated if it gives results in an allowable limit of accuracy[7), 8)]. In the 3-D lattice Model, a concrete column is modelled by the assembly of each orthogonal four truss planes. Each truss plane has an arch element. The thickness of the arch element is decided separately inside each truss by minimisation the total potential energy for each truss plane. The calculation of minimising the total potential energy is carried out at all loading stages[12)].

The solid concrete cross-section column is simulated to a hollow cross-section with a wall thickness "t_w" which is suggested by Hsu[15)]. Since the Lattice Model assumes the compatibility condition and the equilibrium condition, it gives one of the lower bound solutions within the limit of the constitutive model of materials. So, several constitutive concrete curves are investigated to get the suitable softening model for the suggested 3-D lattice Model.

Finally, several theories, like the skew bending theory[5)], space truss theory[19)] and ACI method[7)], in addition to the JSCE equation[18)] and many other code regulations are selected to compare the numerical results using the suggested 3-D Lattice Model. Moreover the numerical results using the suggested 3-D Lattice Model show a successful comparison with the experiment results.

2. MODELLING CONFIGURATION FOR THE 3-D LATTICE MODEL

To analize the reinforced concrete column under pure torsion by the 3-D lattice Model, the most appropriate configuration of Lattice members should be decided. The conceptual idea of space Lattice is explained as in the following. The outside dimensions of the cross-section of the 3-D lattice Model are considered as "b_{eq}" and "d_{eq}", which are equivalent to the outside dimensions of the closed stirrup inside the cross-section of the RC column,

neglecting the surface concrete covering outside the hoop. In the ultimate state, covering concrete is completely spilled off. So, it is only concrete inside the closed stirrups to play dominant role. Since it is putting much emphasis on the ultimate state, the covering concrete outside the stirrups is neglected. In **Fig.1**, within the area of "bd" the column is represented by four simple truss planes, which are orthogonal to each other. Each truss plane follows all the assumptions of the Modified Lattice Model in 2-D as it was suggested previously by the authors[12]. For the stability of this space trusses, there are two cross diagonal members between each of two opposite corner nodes, with a constant area. These elements have not any effect on the output results in case of the pure torsion. In case of reinforced concrete column under pure torsion, which is considered a focus of this study, all the corners of the column is under tensile stresses. Area of the vertical strut equals to the corner area, which is bisected by the equivalent wall thickness, as will be discussed later in section 3 as shown in **Fig.2**. Longitudinal reinforcements are simulated into vertical members, while transverse reinforcements are simulated into horizontal truss members. In each truss plane of the column, Lattice Model has diagonal concrete tension and compression members with the area as shown in **Fig.2**. During the calculation, area of the sub-diagonal member will be calculated after the value of the thickness of the arch element "t" is determined, as it will be explained later in the next section. Two pairs of the diagonal members are considered, as it is suggested before by the authors[9), 10)]. For the trusses in the wider face of the column, the inclination angle of the diagonal members is fixed at 45 degrees. For the other two sides in the short direction, the position of the nodes are kept exactly as they are determined from the wider faces. So, in the short side of the cross-section, the diagonal angles will usually larger than 45 degrees. **Fig.2** shows the cross-section of the 3-D Lattice Model, considering the tension zone area firstly suggested as a square section at each corner zone, with an area equals to $t^2{}_w$. This tension area at each corner zone will be studied clearly in the next section.

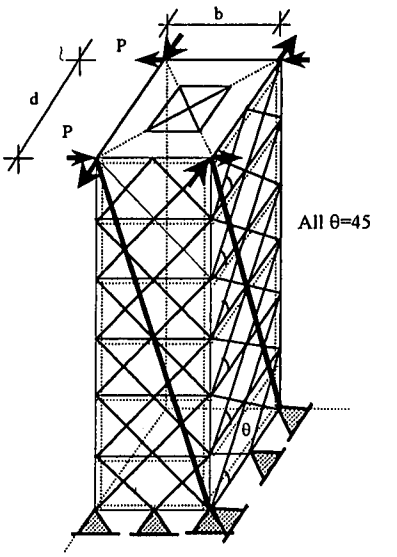

Fig.1 3-D lattice Model for reinforced concrete column

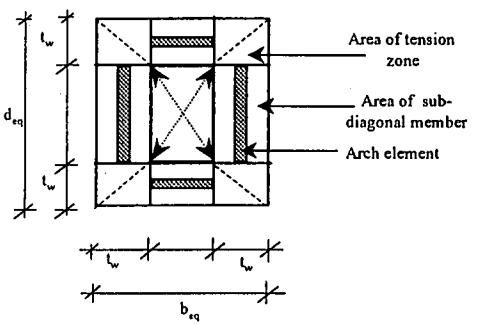

Fig.2 Cross-section of 3-D Modified Lattice Model

3. DETERMINATION OF DIMENSIONS OF TRUSS MEMBERS

(1) Thickness for the wall side

For a reinforced concrete column with a solid cross-section under pure torsion, many researches mentioned that the core of the cross-section does not resist any torsion[15]. Thus the shear flow runs only in a definite thickness at each side of the cross-section. Hsu suggested an equation to calculate this thickness using Eq.(1)[15]. **Fig.3** shows a solid cross-section column and the equivalent hollow cross-section with the effective wall thickness t_w.

$$t_w = 1.2 * A_c / P_c \qquad (1)$$

Where t_w is the wall thickness of the hollow section, A_c is the area of the solid section and equals to $b*d$ and P_c is the outer perimeter of the cross-section and equal to 2(b+d). The appropriateness of this assumption will be explained in the combined discussion of diagonal member effect, arch element and tension zone effects.

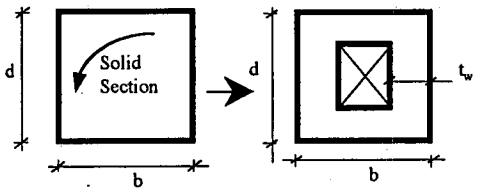

(a) Solid cross section (b) Equivalent hollow cross section

Fig.3 The equivalent solid cross-section with a hollow section

(2) Thickness of the arch element

Fig.4 shows the truss plane in addition to a lateral cross-section for each side of the column. The thick solid line in **Fig.4** represents the arch element, which is connected to the nodes at both ends of the beam with an area as shown in the cross-section in **Fig.4**. In the analysis, the arch element and the diagonal elements are separated and each one of them has its stress and strain distribution[20]. The reason of this element separation is that the structural action is normally a combination of series and parallel couplings of the cracking zones and the uncracked (elastic) zones. In the modified Lattice Model, these zones are simulated with continuous pairs of tension and compression members. The arch member is a key element in this study. It resists the compressive stresses, which is created in each side during torsion especially in the wider face of the column. Normally, the values of the strains or the stresses of the column are not constant along the width of each side in the same cross-section[17]. It means that the stress or the strain is not uniformly distributed in the direction of the width or the depth of each side of the column [17]. So, in the suggested model, the arch element and the diagonal element are separated, and each one of them has its stress and strain distribution. The arch element has the ability to resist a large portion of the applied load. So, it is necessary to simulate it exactly during all the different loading stages.

It is found that the calculation of the total potential energy of the structure has a significant shifting during the calculation[12]. The width of the arch element varies with the change of the load and material deterioration of concrete. It is decided in such a way that the total potential energy becomes minimum value, at which the stiffest case of the structure occuring [12]. So in this study, the total potential energy is calculated for each element of each truss plane, and for different values of factor "α", where the final value of the width of the arch

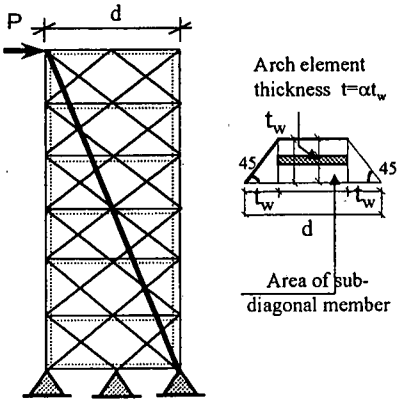

(a) Schematic diagram (b) Cross-section

Fig.4 Two dimensions Lattice and its cross-section

element "t" equals αt_w. α in the calculation starts from 0.1 up to 0.9 with a very small increment. The total potential energy for each truss plane is calculated using Eq.(2).

$$T.P.E. = \sum_{i=1}^{n} f_i \delta_i - P\Delta \qquad (2)$$

In this equation, *T.P.E.*, is the total potential energy for each of plane truss, f_i is the internal force inside each element of the truss side, δ is the displacement of each individual member, n is the number of the truss members, P is the value of the external load applied at the top column or the top of the truss planes as shown in **Fig.4** and Δ is the displacement at the loaded point. By minimising these values of the total potential energy, we can get the corresponding "α" value at each step of the calculation.

The thickness of the plane, which include truss and arch, is kept constant as t_w, which is given by Eq.(1). The dimension of the square tensile zone effects the dimension of the arch depth. By changing the side length of the square tensile zone, the effect of those dimensioning is investigated. The area of the tension zone is firstly suggested being equal to t^2_w, as a small square at each corner. Then the square area of 0.5, 1.0 and 1.5 times of the value t^2_w are analysed as a separate cases for the tension zone area. In each case, the wall thickness t_w is kept constant, but the area of the tension zone is changed by decrease or increasing the depth of the arch element at each side.

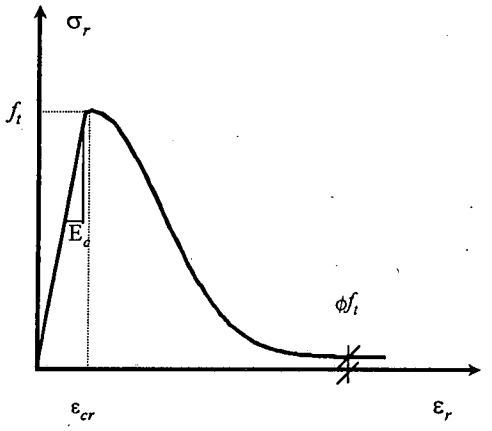

Fig.5 Tensile stress-strain curve of concrete

4. CONSTITUTIVE EQUATIONS

In the Modified Lattice Model the diagonal tension member of concrete resists the principal tensile stress resulting from shear force. The stress-strain relation of tension member of concrete has been taken as expressed in Eq.(3) and Eq.(4)[13] and as shown in **Fig.5**.

For ascending branch $(\varepsilon_r < \varepsilon_{cr})$

$$\sigma_r = E_c \varepsilon_r \tag{3}$$

For descending branch $(\varepsilon_r \geq \varepsilon_{cr})$

$$\sigma_r = (1-\phi) f_t \exp\left[-m^2\left(\frac{\varepsilon_r}{\varepsilon_{cr}}-1\right)^2\right] + \phi f_t \tag{4}$$

Where ε_r and σ_r are the strain and the stress of the tension element respectively. ε_{cr} is the strain at the cracking of concrete and E_c is the modulus of elasticity of concrete. The stress-strain behavior of concrete in tension is elastic before cracking and exhibits softening after cracking. The softening slope should take care of fracture energy for plain concrete and tension-stiffening effect for reinforced concrete[13]. Eq.(3) shows the elastic behavior before cracking. In Eq.(4) m can be varied to simulate appropriate fracture energy for plain concrete. Appropriate ϕ can be chosen to simulate the residual stress in the final stage of damage for simulating tension-stiffening effect in reinforced concrete[13]. In this research m=0.5 and ϕ =zero are adopted. The fracture energy of concrete is assumed to be equals 100N/m. For the reinforcing bars, the stress-strain relationship is assumed to be elasto-plastic for the case of tension and compression members.

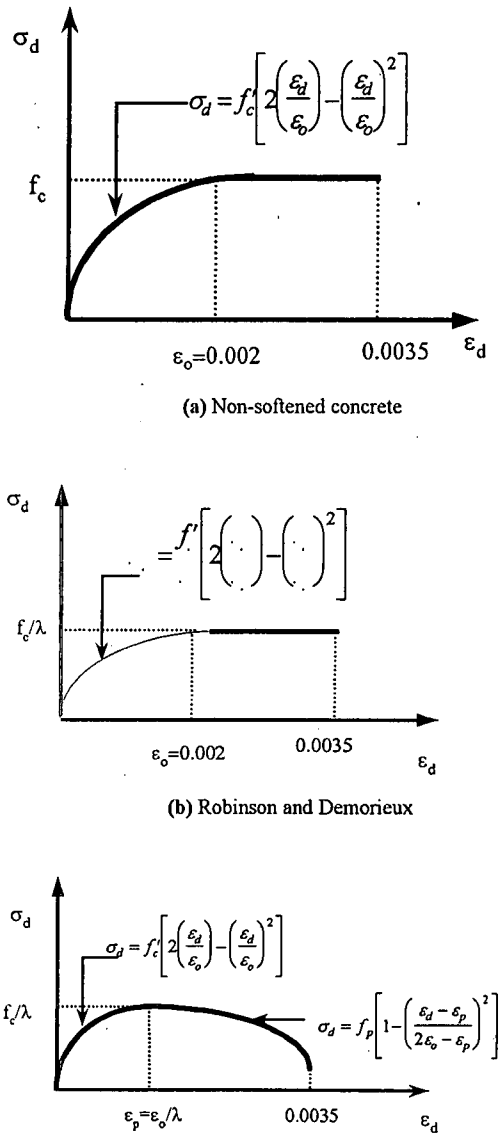

Fig.6 Stress-strain curves for softened concrete

The stress-strain curve of softened and non-softened concrete is studied, to get the suitable softening model for the 3-D lattice Model. For non-softened concrete, the stress-strain curve is based on the standard cylinder tests. For simplicity the parabola-rectangle curve in **Fig.6 (a)**, specified by the CEB-FIP[4] model code is used. The equation for

the parabolic portion of the curve is shown in Eq.(5).

$$\sigma_d = f_c'\left[2\left(\frac{\varepsilon_d}{\varepsilon_o}\right) - \left(\frac{\varepsilon_d}{\varepsilon_o}\right)^2\right] \quad (5)$$

Where,

σ_d is the stress in the diagonal concrete strut.

ε_d is the strain in the diagonal concrete strut.

f_c is the maximum compression stress for the standard concrete cylinder.

ε_o is the strain at the maximum compressive stress

Robinson-Demorieux stress-strain curve for softened concrete is also studied[21], which can be idealised as shown in **Fig.6 (b)**. This stress-strain curve is obtained by dividing the concrete cylinder strength by a coefficient λ, which is greater than unity. For the ascending portion of the curve the equation is as Eq.(6).

$$\sigma_d = \frac{f_c'}{\lambda}\left[2\left(\frac{\varepsilon_d}{\varepsilon_o}\right) - \left(\frac{\varepsilon_d}{\varepsilon_o}\right)^2\right] \quad (6)$$

The portion of this curve after reaching the maximum stress remains horizontal. As compared to the CEB-FIP Stress-Strain curve for non-softened concrete, the stress in this stress-strain curve has been proportionally scaled down by λ, but the strain has not been modified. The Coefficient λ in Eq.(6) was not determined by Robinson. So, that λ which is suggested later by Vecchio and Collins, as it will be shown below is used in this case.

Vecchio and Collins stress-strain curve for softened concrete shown in **Fig.6(c)** is also studied [22]. For the ascending portion of the curve the equation is as shown in Eq.(7).

$$\sigma_d = f_c'\left[2\left(\frac{\varepsilon_d}{\varepsilon_o}\right) - \lambda\left(\frac{\varepsilon_d}{\varepsilon_o}\right)^2\right] \quad (7)$$

Eq.(7) is identical to Eq.(6) except that a coefficient λ has been inserted in the second term. This Coefficient λ, which incorporated the softening effect, was found from tests to be as in Eq. (8)[15].

$$\lambda = \sqrt{\frac{2\,\varepsilon_l\,\varepsilon_t}{(\varepsilon_d)^2}} - 0.3 \quad (8)$$

Where

ε_l is the strain in the longitudinal bars, and ε_t is the strain in the transverse hoop bars. The softening effect is related to the longitudinal and transverse strains in the reinforcement. Beyond the peak strength and in the descending portion of the stress-strain curve (i.e. $\varepsilon_d > \varepsilon_p$), the expression of the curve follows Eq.(9).

$$\sigma_d = \frac{f_c'}{\lambda}\left[1 - \left(\frac{\varepsilon_d - \varepsilon_p}{2\varepsilon_o - \varepsilon_p}\right)^2\right] \quad (9)$$

5. APPROPRIATE DISCRETIZATION METHOD FOR THE 3-D LATTCIE MODEL

(1) Effect of the arch element

Arch element has an important effect on the results in the 3-D lattice Model. To prove this effect, column C_7 in **Table 1** is analyzed two times, one with the effect of arch element and the other without arch element. **Fig.7** shows the relation between the torsion moment and the angle of twist for the two cases comparing with the experimental data. From this figure, the attendance of the arch element has not a significant effect on the cracking torque, since the value of the cracking torque is almost same for the two cases. But the main effect happens after the cracking. Even the ultimate torque decreases too much in the second case without arch element. As the value of the compression force of the arch element is considered a little pit small at the cracking load. So, the arch element as a compression member has not any segneficant effect before the cracking of the column. From the outpot results, the effect of the arch element starts from the initiation of cracking up to the final torque.

(2) Effect of the area of the tension zone

To study the effect of the area of the tension zone at each corner, three different values for this area are studied *as* $0.5t^2_w$, t^2_w and $1.5t^2_w$. **Fig.8** shows the torsion moment and the corresponding angle of twist for the column C_7 group B in **Table 1**, considering all the three different suggested values for the tension zone area. In this figure a comparison between the numerical results and the experimental results are shown. The relation between the torsion moment and the corresponding angle of twist becomes higher than the experimental results in case of the tension zone equal to $1.5t^2_w$. However, it becomes lower the experimental results in case of area equals half of t^2_w. Further more, the cracking load decreased lower than that of the experimental value in this case. That is for the decrease of the elastic energy with the decrease of the stiffniess of the structure. Before the cracking

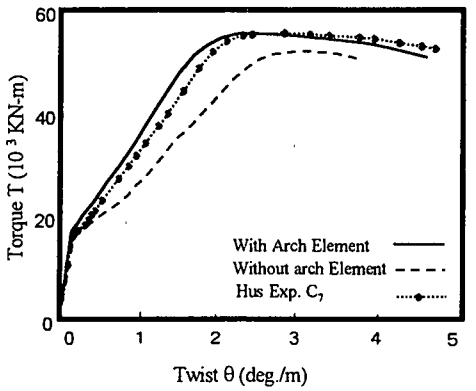

Fig.7 Torque-twist curve for C_7 with/ without arch element

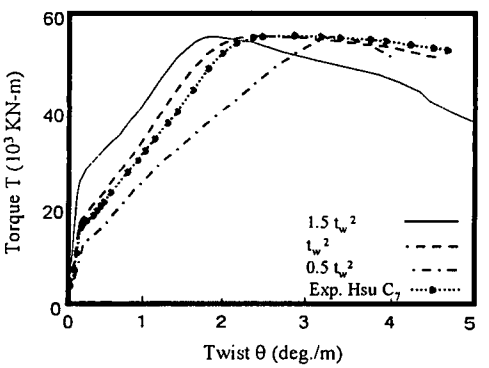

Fig.8 Torque-twist curves for C_7 with different tension zone areas

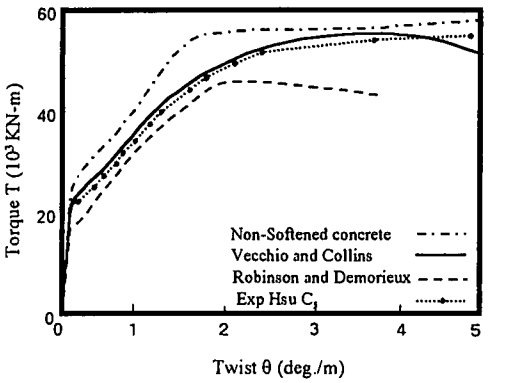

Fig.9 Torque-twist curves for different softening

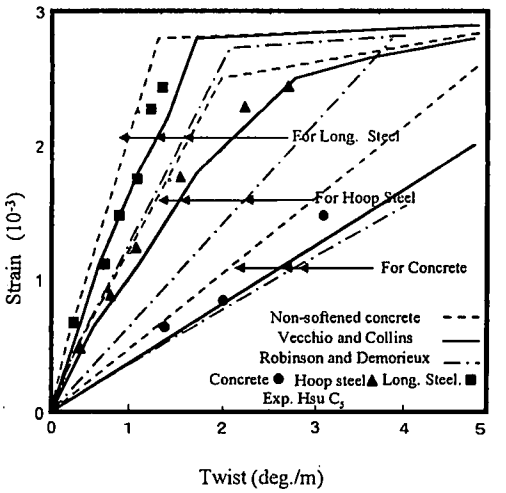

Fig.10 Strain-twist curves for column C_5

occurs, there is no significant difference between the numerical results and the experimental results using the three different values, because in this stage the structure considered like a plain concrete section. However, the cracking torque is changed sharply. After yielding, there is a significant effect for changing the tension zone area, but there is no significant difference on the ultimate torque. The angle of twist at the ultimate torque is changed too much in between the three different area values. From **Fig.8**, it is found that the numerical results have a good agreement when the area of the tension zone equals to $t^2{}_w$. So, it will be kept constant as $t^2{}_w$ for all the next calculations in this study.

(3) Analysis of the different softening equations

Using the different softened and non-softened stress-strain curves, which are suggested, in section 4, column C_5 in **Table 1** is analysed and compared with the experimental results. **Fig.9** shows a comparison between the three cases of non-softened and softened concrete. The comparison is carried out to show the relation between the torque and the angle of twist for the column C_5. The steel-strain versus concrete-strain curve for column C_5 is also shown in **Fig.10** using the previous three cases of the softened behaviour. From **Fig.9**, Robinson and Demorieux's stress-strain curve could neither produce accurate predictions of angle of twist at maximum torque nor the shape of the torque-twist curve. By comparing the numerical results with the experimental results as it is shown in the last two figures, it is clear that the Vecchio and Collins softened fits the behaviour of the numerical results using the 3-D Lattice Model with a good agreement comparing with the experimental data.

Table 1 Outline of the experimental results

Group	Number	cross-section m	Fc Concrete MPa	Fly for Reinf MPa	Fsy for Stirrups MPa	Long Bars #	Stirrups Bar s, m.
A	C_1	o.255/0.383	31.0	490.0	530.0	4#4	#3 at 0.153
A	C_2	o.255/0.383	31.0	490.0	530.0	4#5	#4 at 0.182
A	C_3	o.255/0.383	31.0	490.0	530.0	4#6	#4 at 0.128
A	C_4	o.255/0.383	31.0	490.0	530.0	4#7	#4 at 0.092
A	C_5	o.255/0.383	31.0	490.0	530.0	4#8	#4at 0.070
A	C_6	o.255/0.383	31.0	490.0	530.0	4#9	#4 at 0.057
B	C_7	o.255/0.383	28.0	480	505	4#4	#4 at 0.128
C	C_8	0.5/0.60	38.5	510.0	510.0	10#8	#4 at 0.050
D	C_9	0.222/0.222	39.6	380.0	285.0	4#3	#2 at 0.080
D	C_{10}	0.146/0.324	36.3	380.0	285.0	4#3	#2 at 0.083
E	C_{11}	0.441/0.441	27.5	414	414	8#5	#3 at 0.08
E	C_{12}	0.312/0.625	27.5	414	414	8#5	#3 at 0.08
E	C_{13}	0.255/0.765	27.5	414	414	8#5	#3 at 0.08

6. BEHAVIOURE OF THE RC CULUMNS UNDER PURE TORSION

After establishing the appropriate choice of concrete constitutive equation and dimensioning of each lattice member, different RC columns are analysed and compared with the experimental data. **Table 1** shows the experimental data for several kinds of the compared cross-section columns. Columns in-group A tested by Hsu[16] are identical except that the amount of reinforcement increases from C_1-C_6. Column C_7, group B tested by Hsu[16] is similar to the group A but with a different ratio of longitudinal reinforcement to stirrups area. Column C_8 represents a group C tested by Hsu[15], is an example for the large hollow cross-section column with a wall thickness equals $0.11m$. Columns C_9 and C_{10} in-group D tested by Arthur[3], are an example for small size cross-section columns. C_9 and C_{10} are identical except the change in the cross-section area. Finally, columns in-group E tested by Arthur[3] represents the columns C_{11}-C_{13} have the same cross-section area of concrete and reinforcements, but with different aspect ratios.

Fig.11 shows the relation of the torsion moment and the angle of twist for the columns C_1-C_6 group A in **Table 1**. Also, several kinds of cross-sections like a hollow cross-section as well as small size cross-sections are analysed, as it will be mentioned later in the next section. The behaviour of the reinforced concrete columns subjected to pure

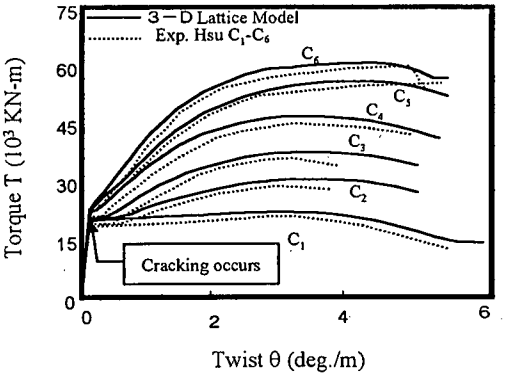

Fig.11 Torque-Twist Curves for columns group A in **Table 1**

torsion can be divided into two distinct stages, before and after cracking of the concrete. Before cracking, a column behaves essentially as a plain concrete column without reinforcement. The stress in the reinforcement is small, and the torque-twist curve is almost identical to that of a plain concrete column. When the cracking of concrete occurs, the stresses in the reinforcement increase suddenly and the column twisted under constant torque until it reaches a new state of equilibrium. Thereafter, the applied torque can be further increased, but the stiffness of the column is only a fraction of that before cracking.

(1) Behaviour before cracking

It is found that the cracking torque, T_{cr}, of a reinforced concrete column is 1.0 to 1.25 times the failure torque of its corresponding plain concrete column. This strengthening is apparently due to the reinforcement, and it should increase with the increasing amount of reinforcement. In this stage, the torsional stiffness and the concrete strains were also very close to those of the corresponding plain concrete columns. Also it is found that, at the cracking torque, the stresses in the reinforcement increased suddenly.

(2) Behavior after cracking

As described above, a reinforced concrete column behaves before cracking like a column without reinforcement, it follows approximately Saint-Venant's elastic torsional theory. However Saint-Venant's theory was often not accurately applied by many investigators to predict the behaviour of reinforced concrete columns after cracking. For example, according to such application of saint- Venant's theory, the stresses in the longitudinal bars located at the four corners of a rectangular cross-section should be zero, while stresses in bars located at the wider face should be a maximum. The analysis results using the 3-D Lattice Model shows that, these stresses are essentially equal regardless of the location of the longitudinal bars. Similarly, the theory predicts that stresses in a closed stirrup should vary from zero at the shorter leg to the maximum at the centre of the longer leg. Here using the 3-D Lattice Model it is found that, the stresses are almost similar for both of the two steel stirrup elements along the depth of the column. Here, it must be concluded, therefore, that Saint-Vaenant's theory cannot applied to a reinforced concrete column after cracking, because cracking terminates Saint-Vaenant's basic assumption that the material is continuous.

a) General behaviour

Columns in-group A are identical except that the amount of reinforcement increases from the first column up to the last one, as shown in **Table 1**. **Fig.11** shows that, upon cracking, the angle of twist increased significantly under a constant torque. As a common behaviour in all cases, the stresses in the reinforcement increased suddenly after the cracking occurs. In case of beam C_1, which has a very small amount of reinforcement, the angle of twist under constant torque after cracking was very large, and the stresses in the reinforcement increased almost to the yield point. However, as the curves for other columns show that, the angle of twist and steel stresses immediately after cracking decrease with increasing amount of reinforcement. The torque-twist curves in **Fig.11** show that, when a column stabilised after cracking, the curve begins to rise again. It was first essentially as a straight line, then curved towards the horizontal when the ultimate torsion was approaches. The slope of the slope portion, which is the torsional stiffness after cracking, is only a fraction of that before cracking. It increased with increasing amount of reinforcement from column C_1 up to C_6. At the same time the stresses in the steel is changed approximately and increased regularly from C_1 up to C_6.

b) Ultimate torque

Ultimate torque is defined as the maximum torque, which can be resisted by the member. This value depends on a large extent on the amount of reinforcement, as shown in **Fig.11**. At the ultimate torque, the stresses in the longitudinal bars and in the longer legs of the stirrups can both reach the yield point when small percentages of reinforcement are used, such as columns from C_1 to C_3. However, they cannot reach yielding with a large percentage of reinforcement, such as column C_6 in **Fig.11**. This means that columns C_1-C_3 are under-reinforced and column C_6 is over-reinforced. For columns C_4 and C_5 the longitudinal bars yielded, but the stirrups did not. This indicates that these columns are over-reinforced in stirrups only. In case of over-reinforced section, failure occurs by initial crushing of the concrete. At the initiation of failure, the steel strain will be lower than the yield strain. Such condition is accomplished by using more reinforcement at the tension side than that required for balanced condition. But in case of under-reinforced section, steel continues to stretch as steel strain increases beyond the yielding strain. This condition is accomplished when the area of the tension reinforcement used in the beam is less than that required for balanced strain section

Beyond the ultimate torque, **Fig.11** shows that the torque-twist curves exhibited a definite descending branch for columns C_1-C_3. In general, the descending branches of the torque-twist curves for under-reinforced columns were longer than those for curves of over-reinforced columns, which terminated shortly beyond the maximum torque.

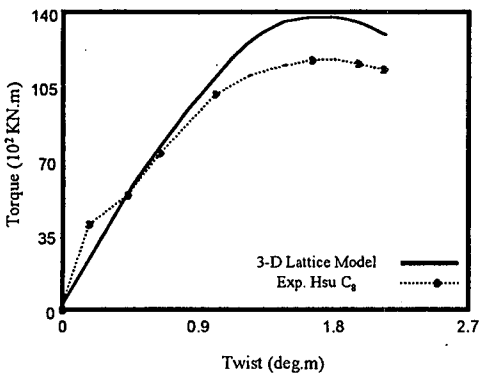

Fig.12 Torque-Twist curve of hollow Cross-section column C_8

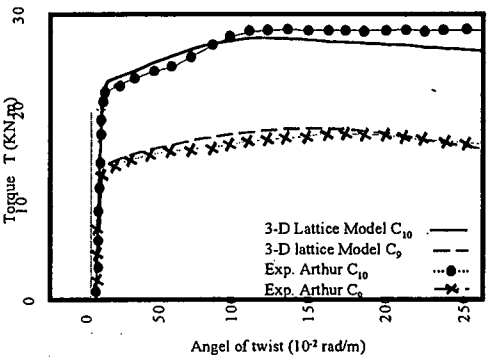

Fig.13 Torque-Twist curves for small sections group D in **Table 1**

7. APPLICATION FOR SPECIAL CASES OF CROSS-SECTIONS

Hollow cross-section column C_8 group C in **Table 1** is analysed by the suggested 3-D Lattice Model. The numerical and the experimental results are shown in **Fig.12**. In this figure, the ascending portion of the analysed torque-twist curve lies considerably upper the test results as shown in **Fig.12**. The reason for this discrepancy is obvious. Although the 3-D Lattice Model is based on the truss theory-which is assumed to be fully cracked from the beginning-it has the arch element, which has the ability to carry a high-level of loading. After cracking, arch element will continue to stiffen the specimen to reach the fully cracking at the maximum torque. This behaviour is quite similar to the solid section.

Moreover, small size cross-section columns are also analysed by the 3-D Lattice Model. Cross-section columns C_9 and C_{10} group D in **Table 1**, are chosen as an example for this case, to be analysed. The numerical and the experimental results are shown in **Fig.13**. In this kind of cross-section column, cracks appeared firstly in the large faces of the columns, and soon thereafter spiralled around all faces of the columns. The cracking torque is defined as the torque at which the first crack occurs. At the cracking torque in **Fig.13**, the torque –twist curves show an increase in twist at a virtually constant torque. This horizontal part of the curve indicates a change in the load carrying mechanism of the columns at cracking.

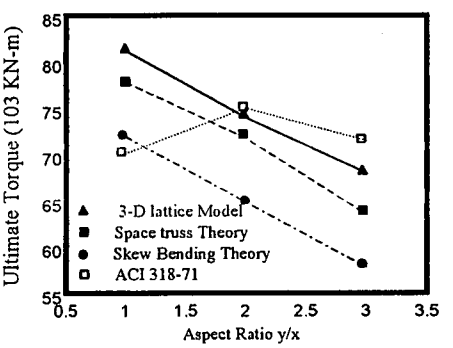

Fig.14 Effect of aspect ratio on the ultimate torque

8. COMPARISON WITH THE PREVIOUS THEORIES

As a comparison with different approximation theories, we pick up the space truss theory[19], skew bending theory[5] and ACI method[2], and try to analyze the column with a quite large aspect ratio. The effect of the aspect ratio is considered a very important factor during the design of column under the pure torsion. Both the skew bending theory and the space truss theory predicted that the ultimate torque would decrease with an increase in the aspect ratio, whereas the ACI method predicts an increase initially and then a decrease. To show this effect using the 3-D Lattice Model, three columns C_{11}, C_{12} and C_{13} group E in **Table 1** are considered with different aspect ratios. 1.0, 2.0 and 3.0 only of the aspect ratio for the columns C_{11}, C_{12} and C_{13} respectively as in **Table 1**, are analysed. The trends, which predict the ultimate torque of the three different methods, are shown in **Fig.14**. The ACI method predicts that the square

section is the weakest among the other columns, whereas the other two methods predict it to be the strongest section. **Fig.14** shows the ultimate torque computed by the skew bending theory, space truss theory, and ACI 318-71 comparing with the 3-D lattice Model, for the three different columns. Although all the three theories underestimate the strength of all the beams, that trend, which predicted by ACI 318-71 is contradictory to the numerical, results from the suggested Model. So, the torsional stress of a column decreases with an increase in aspect ratio, other parameters being held constant.

9. COMPARISON WITH THE CURRENT CODE REGULATIONS

To check the applicability of the various code regulations, the numerical results are compared with some of the existing codes. According to the German[14] and Australian[1] codes, the equation for ultimate torque is shown in Eq.(10).

$$T_u = T_o + \Omega x_1 y_1 \frac{A_s f_{sy}}{S} \qquad (10)$$

Where

T_u = ultimate torque

T_0 = In the Australian Code is the failure torque of the beam without reinforcement according to Saint-Venants theory.

T_0 = zero in the German code

Ω = a constant, 2 and 1.6 for the German and Australian codes, respectively

x_1 = smaller centre-to centre dimension of a closed rectangular stirrup

y_1 = larger centre to centre dimension of a closed rectangular stirrup

A_s = cross-section area of one stirrup leg

f_{sy} = yield strength of stirrups

S = spacing of stirrups

Using the 3-D lattice Model, the ultimates torque for columns C_1-C_6 are plotted against the parameter $x_1y_1(A_sf_{sy}/S)$ as shown in **Fig.15**. It can be seen that the relationship is a strait line through points C_1 up to C_3, then turns gradually toward the horizontal. The whole curve can be approximately divided into three strait segments as shown by the dotted lines. The first straight line through points C_1 to C_3 corresponds to under-reinforced columns, where both the longitudinal bars and the longer legs of the stirrups yielded before the ultimate torque was reached. This condition is accomplished when the area of the tension reinforcement used in the beam is less than that required for balanced strain section. The second straight portion through points

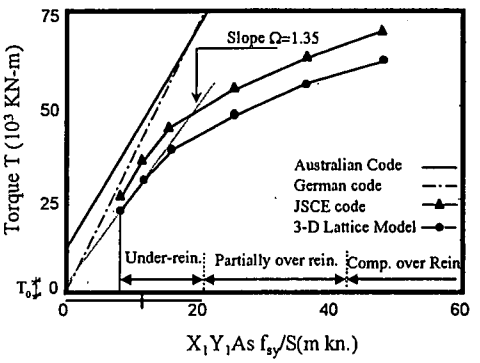

Fig.15 Comparing the ultimate torque with other codes

C_4 and C_5 corresponds to partially over reinforced columns in which the stirrups did not yield. The last horizontal line through point C_6 corresponds to completely over reinforced columns, where neither longitudinal bars nor stirrups yielded, so that failed by primary crushing of the concrete. In this case the steel stress will be lower than its yield strength. Such condition is accomplished by using more reinforcement at the tension side than that required for balanced condition. Eq. (11) shows the balanced reinforcement ratio for a RC section.

$$\rho = \beta \frac{0.85 f_c'}{f_y} \frac{87000}{87000 + f_y} \text{ (in psi)} \qquad (11a)$$

$$\text{where } \beta = \begin{cases} = 0.85 \, for \, 0 < f_c' \le 4000 psi \\ = 0.85 - 0.05\left(\dfrac{f_c' - 4000}{1000}\right) \\ for \, 4000 psi < f_c' \le 8000 psi \\ = 0.65 \, for \, f_c' > 80000 psi \end{cases} \qquad (11b)$$

and f_c' is the compressive stress for the concrete section.

For under reinforced columns, the parameter A_sf_{sy}/S appears to be acceptable. The slope, Ω, of the first straight portion is 1.35, and the ultimate torque can be expressed by Eq.(10). The prediction of the German and Australian codes are also plotted in **Fig.15**. It can be seen that the observed "T_0" be smaller than that predicted by the Australian codes, but larger than that of the German codes. T_0 be commonly thought to be the torsional resistance of the concrete section.

The applicability of the suggested 3-D Lattice Model is examined also by the JSCE codes[18]. The ultimate torque for the studied columns group A in **Table 1**, is calculated by the 3-D Lattice Model and also compared using JSCE Eq.(12).

$$M_u = 2A_m\sqrt{q_w q_l}/\gamma_b \quad (12)$$

$$q_w = A_{tw} f_{wd}/S \quad (12a)$$

$$q_l = \sum A_{tl} f_{ld}/u \quad (12b)$$

$$u = 2(b+d) \quad (12c)$$

Where, M_u is the ultimate torque, $A_m = bd$ of the cross-section, A_w and A_t are the areas of the lateral and longitudinal steel respectively, f_{wd} and f_{ld} are also the yield stresses for the lateral and longitudinal steel respectively and $\gamma_b = 1.3$ in general. The comparison is shown also in **Fig.15.** The tendency of the prediction by the suggested 3-D Lattice Model is not necessary similar to Eq.(12). The ratio is varied around $\pm 5\%$, which is considered an adequate ratio.

10. CONCLUSION

The Modified Lattice Model, which is suggested before by the authors, is extended to the three dimensions. 3-D Lattice Model consists of four simple trusses; each one has its arch element. Thickness of the arch element is calculated inside each truss by minimising the total potential energy for all the members of the truss. Its value is updated inside each step of the calculation during all the different loading stages. The solid cross-section of the RC column is chosen as a subject material to check the applicability of the 3-D lattice Model. The equivalent thickness value t_w for the walls, which is suggested by Hsu, is implemented in this model. Area of the tension zone at each corner of the cross-section equals to t^2_w, at which the results become closer to the experiment results, comparing with several other values. Using the suggested model, the effect of several softened and non-softened concrete curves are studied to get the most suitable curve for the 3-D Lattice Model. Vecchio and Collins stress-strain is the most suitable softening concrete curve, at which the numerical results becomes more closer and has a good agreement with the experimental data. Several RC columns are analysed under the pure torsion using the suggested 3-D Lattice model. The numerical results are compared with the experimental results; there is a good agreement with an adequate ratio. The behaviour of the RC columns under pure torsion is studied. RC column before cracking, behaves essentially like the plain concrete section without effect of the reinforcement, since the stresses in the reinforcement is very small. However, after cracking it does not follow Saint-Venant's theory because the material at this stage is not continuous.

The effect of the aspect ratio is studied comparing with the skew bending theory, the space truss theory and the ACI method. The 3-D lattice Model predicts a decrease of the ultimate torque with the increase of the aspect ratio. This behaviour is kept common for all the skew bending theory, apace truss theory and the 3-D Lattice Model, in contrast with the ACI method.

Finally, The applicability of the 3-D lattice Model is compared by the Australian and German codes, in addition to the JSCE equation. The behaviour is always lower than these codes, which gives the results more safety. The predicted ratio using the JSCE equation is varied with $\pm 5\%$, which is considered an acceptable ratio.

REFERENCES

1) Australian code: SAA code for concrete in building, Australian Standard, No. CA.2-1958, standard association of Australia, Sydney, pp. 109, 1958.
2) ACI Committee 318: Building code requirements for reinforced concrete (ACI 318-71), American concrete institute, Detroit, PP. 78, (plus cumulative supplement issued annually), 1971.
3) Arthur E. McMullen and B. Vijaya Rangan: Pure torsion in rectangular sections- a re-examination, ACI Journal, No. 75-52, pp. 511-519, Oct. 1978.
4) Committee Euro-International: CEB-FIP Model code for concrete structures, 3rd Edition, du Beton/Federation International de la Precontrainte, Paris, pp. 348, 1987.
5) Collins, M. P., Walsh, P. F. Archer, F. E. and Hall, A. S.: Reinforced concrete in torsion, UNICIV report, No. R-31, University of New south Wales, Kensington, Australia, pp. 328, 1968.
6) Choi, I.K. and Niwa, J.: Analytical study on shear behavior of concrete beams by Lattice model, proc. of JCI, Vol. 16, 1994, (In Japanese).
7) EL-Behairy, F.M. Niwa, J. and Tanabe, T. A.: Analytical study on pure torsion behavior of concrete columns using 3D-Lattice Model, Proc. JCI, Vol.18, No.2, pp. 263-268, 1996.
8) El-Behairy, F.M., Niwa, J. and Tanabe, T. A.: Simulation of the R.C. column behavior in 3D- stress state under pure torsion using 3D-Lattice Model, Proc. of JCI Transaction, Vol. 18, pp. 303-309, 1996.
9) EL-Behairy, F.M. and Tanabe, T. A.: A new technique for reinforced concrete beam analysis using the Modified Lattice Model, Proc. of JCI, Vol. 19, No.2, pp. 477-482, 1997.
10) EL-Behairy, F.M. and Tanabe, T. A.: Rational discretization method for reinforced concrete beam analysis using the Modified Lattice Model, Proc. of JCI transaction, Vol. 19, pp. 365-372, 1997.
11) EL-Behairy, F.M., Niwa, J. and Tanabe, T. A.: Application of the Modified lattice model to simulate

shear failure of the RC beams, Proc. of JCI Vol. 20 No. 3, pp. 361-366, 1998.

12) EL-Behairy, F.M., Niwa, J. and Tanabe, T. A.: A study on the fundamental characteristics of lattice Model for reinforced concrete beam analysis, Journal of japan coc. Civil Eng. (JSCE), Journal of materials, concrete structures and pavements, No. 599/V-40, august 1998, pp. 165-175.

13) EL-Behairy, F.M. and Tanabe, T. A.: Development of the lattice Model and its application for the shear failure mechanism, International conference CIB World Building Congress, Gavle, Sweden, June 7-12, 1998.

14) German Standard code, Bemessung im stahlbetonbau: Design of reinforced concrete, DIN 4224, Wilhelm Ernest and Sohn, Berlin, pp. 57, 1958.

15) Hsu, Tomas T. C. and Y. L. Mo: Softening of concrete in torsional members-theory and tests, ACI Journal No. 82-25,1985

16) Hsu, Tomas T. C.: Torsion of structural concrete-Behavior of reinforced concrete rectangular members, ACI Publication, *Torsion of structural concrete,* SP-18-10, 1989.

17) Ichinose, T. and Hanya K.: Three-dimensional shear failure of RC columns", *Concrete Under Severe Conditions Environment and Loading*, Vol.2, Edited by K. Sakai pp. 1737~1747, 1995.

18) JSCE, C.L.SP.1, "Standard Specification for Design and Construction of Concrete Structures", First Edition, part 1 (design, pp. 65~69, 1986.

19) Lampert, P. and Collins, M. P.: Torsion, bending, and confusion- An attempt to establish the facts, ACI Journal, proceeding V. 69, No. 8, pp. 500-504, Aug. 1972.

20) Minami K.: "Limit Analysis of Shear in Reinforced Concrete Members", Proc. of JCI Colloquium on Shear Analysis of RC Structures, June 1982.

21) Robinson, J. R. and Demoriex, J. M.: Essais de traction-compression sur modeles d'ame de poutre en beton arme, Institute de Recherches appliquees du Beton (IRABA) part 1, June 1968 and part 2, may 1972.

22) Vecchio, F. and Collins, M. P.: Stress-strain characteristics of reinforced concrete in pure shear, Final report, *IABSE colloquium on advanced mechanics of reinforced concrete*, International association for Bridge and Structural Engineering, Zurich, pp. 211-225. (Delft 1981).

(Received August 10, 1998)

3次元修正格子モデルを用いた純ねじりを受ける鉄筋コンクリート柱の解析

Fawzy Mohamed EL-BEHAIRY・二羽淳一郎・田辺忠顕

本研究では，鉄筋コンクリート柱の挙動をより深く理解するための数値シミュレーションを行う．任意の荷重を受ける構造系の解析は，材料における物理的特性を厳密に取り入れた場合，特に自由度数の増大を引き起こすために非常に困難を有する．そこで本研究では，著者らが以前提案した2次元格子モデルを3次元に拡張し，純ねじりを受けるＲＣ柱の解析を行った．解析結果を多くの実験結果と比較した結果，広範囲にわたる一致が認められ，このモデルの有効性が確認された．